High packing density laser diode stack arrays using Al-free active region laser bars with a broad waveguide and discrete copper microchannel-cooled heatsinks

Zhigang Liu (刘志刚)*, Gaozhan Fang (方高瞻), and Kecheng Feng (冯克诚)

School of Science, Changchun University of Science and Technology, Changchun 130022

E-mail: zgliu@bj163.com

Received June 23, 2008

A high packing density laser diode stack array is developed utilizing Al-free active region laser bars with a broad waveguide and discrete copper microchannel-cooled heatsinks. The microchannel cooling technology leads to a 10-bar laser diode stack array having the thermal resistance of 0.199 °C/W, and enables the device to be operated under continuous-wave (CW) condition at an output power of 1200 W. The thickness of the discrete copper heatsink is only 1.5 mm, which results in a high packing density and a small bar pitch of 1.8 mm.

OCIS codes: 140.0140, 140.2010.
doi: 10.3788/COL20090703.0214.

High power laser diode arrays (LDAs) are widely used for pumping Nd:YAG solid-state lasers[1−3], pumping ytterbium-erbium doped fiber amplifiers (YEDFAs)[4,5], soldering, material processing, and medical therapy. In order to achieve higher power, high reliability, and high efficiency, the use of Al-free materials for the active region has many advantages over conventional Al-containning materials. Al-free materials exhibit lower surface recombination velocity, which results in higher catastrophic optical mirror damage (COMD) and better reliability. Another approach to achieve higher power and high reliability of laser diodes (LDs) is to reduce the optical intensity at the facets. A large optical cavity structure, which increases the 0th transverse mode width, effectively spreads the intensity over a large area and reduces the intensity at the facets. The compact size and the high output power of these devices result in extremely high heat fluxes ($\sim$ 1 kW/cm^2) at the interface where the diode bar is soldered to the heatsink. In order to increase the output power levels of LDAs, many advanced microchannel-cooled heatsinks have been developed to remove so large waste heat from diode bars and keep the bar junction near room temperature. The microchannel-cooled heatsinks can be broadly categorized in two groups: the monolithic microchannel-cooled heatsinks which are less mature, and the discrete microchannel-cooled heatsinks which are usually used in almost all LDA products[6,7]. The structure of the device with a monolithic microchannel-cooled heatsink is that all diode bars are soldered directly or indirectly to one heatsink. In these devices, very high packing density, which can be indicated by bar pitch, can be easily obtained, but the thermal impedance cannot be decreased satisfactorily. Another structure is that one device comprises several discrete microchannel-cooled heatsinks and an individual diode bar is attached to its own heatsink. For the same packing density, the thermal resistance of the device with discrete microchannel-cooled heatsinks is decreased by $\sim$ 5 times over that of the device with monolithic microchannel-cooled heatsinks. In order to maintain enough mechanical strength to hold their shape of the discrete microchannel-cooled heatsinks during stacking, the thickness of over 1.5 mm is usually designed for continuous-wave (CW) devices. Because of the insulator layer between neighboring heatsinks, the bar pitch of CW stack LDAs is usually $\sim$ 1.8 mm.

Another critical issue is the selection of a heatsink material which has good thermal and mechanical properties and can be easily machined, but no material has an ideal combination of all required properties[8]. Up to now, silicon and copper are most usually used. Silicon has the unique ability to be micro-machined by anisotropic etching, by which extremely narrow microchannels can be obtained. But the major weaknesses of silicon are relatively poor thermal conductance and mechanical properties. Copper offers the advantage of high thermal conductivity and low cost.

In this letter, Al-free InGaAsP active region LDs and diode bars with AlGaAs cladding layers are described. A large optical cavity broadened waveguide structure with small vertical far-field divergence is used. A 10-bar LDA with discrete copper microchannel-cooled heatsinks under CW operation is described. In order to improve the packing density, the thickness of the discrete microchannel-cooled heatsink is reduced to only 1.5 mm while keeping the thermal resistance at 0.199 °C/W. The output power up to 1200 W is produced with the bar pitch of 1.8 mm.

The wafer used to fabricate devices was grown by metal organic chemical vapour deposition (MOCVD). The structure of the wafer is as follows. The substrate was a Si-doped n$^+$-GaAs with Si density of 2×10^{18} cm^{-3}. After growing a 0.5-μm GaAs buffer layer, the following layers were grown successively: 1) 0.8-μm n-$Al_{0.6}Ga_{0.4}As$ cladding layer, 2) 0.6-μm InGaAsP waveguide layer, 3) InGaAsP barriers and the quantum well, 4) 0.6-μm InGaAsP waveguide layer, 5) 0.8-μm p-$Al_{0.6}Ga_{0.4}As$ cladding layer, 6) 0.2-μm p$^+$-GaAs top layer, 7) 20-nm p$^+$-GaAs cap layer. Broad area LDs with stripe widths

1671-7694/2009/030214-03

of 150 μm and diode bars were processed. The 1-cm-wide diode bars consist of sixty 150-μm-wide emitters on 160-μm centers. To reduce the influence of current-spreading, the cap layer has been wet-chemically etched beside the contact stripe. Outside the stripe, an insulator layer (SiO_2) was deposited. A Ti/Pt/Au metal contact was evaporated on the p-side. After wafer thinning, the n-side was metallized. The wafer was cleaved to obtain cavity lengths of 1.5 mm. Low reflection ($R < 5\%$) and high reflection ($R > 95\%$) coatings were formed on the front and the rear facets, respectively.

The stack structure consists of 10 diode bars and is 1 cm long. It generates 120-W CW output power. In this structure, discrete copper microchannel-cooled heatsinks are used and each bar is attached to its own heatsink. In order to increase the packing density, the bar pitch is decreased to 1.8 mm. The thickness of insulator layer between neighboring heatsinks is 0.3 mm and the thickness of discrete copper microchannel-cooled heatsink is 1.5 mm. Because of the required 1200-W CW output power of the total 10 diode bars and electrical-to-optical conversion efficiency of $\sim$ 50%, the heat flux generated by the device is about 700 W/cm^2. Figure 1 shows the high packing density stack LDA with discrete copper microchannel-cooled heatsinks.

Figure 2 shows the package unit including a diode bar, a copper microchannel-cooled heatsink, an insulating layer, and a conductive plate. The laser diode bar is mounted p-side down on the copper microchannel-cooled heatsink. The active region (length $L_{\rm bar} = 10$ mm, width $W_{\rm cavity\_length} = 1.5$ mm), which is near the p side, is a planar heat source. The copper heatsink contains deep rectangular channels of width $W_{\rm ch}$ and depth $H_{\rm ch}$ which carry the coolant, separated by fins of width $W_{\rm f}$. The values of $W_{\rm ch}$, $W_{\rm f}$, and $H_{\rm ch}$ are 150, 100, and 1100 μm, respectively. The channels are under the laser diode bar. The size of the cooled area is 4×10 (mm). The distance

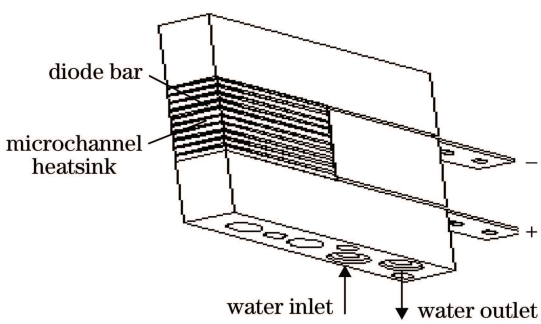

Fig. 1. Schematic diagram of a 10-bar stack LDA with discrete copper microchannel-cooled heatsinks.

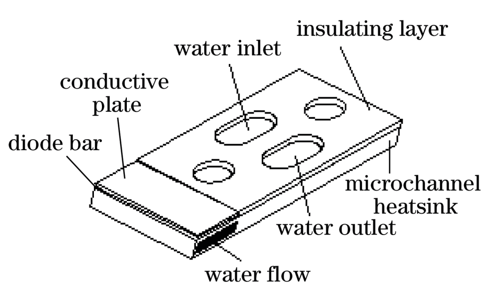

Fig. 2. Schematic diagram of a laser bar package mounted on a copper microchannel-cooled heatsink.

$H_{\rm unch}$ from the top surface of the heatsink to the top of the channels is 0.2 mm. There are 16 parallel channels and the total width $W_{\rm total}$ is 4 mm. The length $L_{\rm ch}$ of the channels is equal to that of the diode bar.

The most important parameter characterizing a LDA package is its thermal resistance $R_{\rm th}$ which is the derivation of the temperature rise ΔT at the diode junction with respect to the dissipated power ΔQ at the junction:

$$R_{\rm th} = \frac{\Delta T}{\Delta Q}. \quad (1)$$

In general, $R_{\rm th}$ is the sum of three components: $R_{\rm cond}$, due to conduction from the active region of the diode bar to the mirochannel interface; $R_{\rm conv}$, due to convection from the microchannel heatsink to the coolant fluid; and $R_{\rm heat}$, due to heating of the fluid as it absorbs heat passing through the mirochannels[9].

The heat flow is conducted from the active region of the diode bar through p-side layer of the bar, the Ti/Pt/Au layer which is the metal layer of the wafer by sputtering, and the indium solder layer. Because the thicknesses of the Ti/Pt/Au layer and the indium layer are very small, the thermal impedance due to the two layers are neglected. The thermal resistance is simply expressed as

$$R_{\rm cond} = \frac{L}{kA}, \quad (2)$$

where L is the conductive length of the heatsink material (L is the thickness $H_{\rm unch}$ of the unchannelled heatsink), k is the thermal conductivity of the heatsink material (390 W/(m·°C) for the copper heatsink), and A is the heat conductive cross section of the heatsink material. The heat flux within the active region is assumed to be uniform and steady-state, so A is simplified as the size of $L_{\rm bar} \times W_{\rm cavity\_length}$. In order to reduce $R_{\rm cond}$, the mirochannels are located very near to the heat source which is the active region of the diode bar. The thickness $H_{\rm unch}$ of the unchannelled heatsink is thinned to 0.1 mm, and $R_{\rm cond}$ is only 0.017 °C/W.

$R_{\rm heat}$ is defined by

$$R_{\rm heat} = \frac{1}{\rho C_p f}, \quad (3)$$

where ρC_p is the heat capacity of the coolant and f is the coolant flow rate. $R_{\rm heat}$ can be reduced by using a coolant of high volumetric heat capacity at a sufficiently high flow rate. ρC_p of water is 4.18 J/(°C·cm^3) and a modest flow rate of each discrete copper microchannel-cooled heatsink is 16 cm^3/s, so $R_{\rm heat}$ is 0.015 °C/W.

In the microchannel heatsink design, the convective thermal resistance $R_{\rm conv}$ is the dominant consideration. $R_{\rm conv}$ is given approximately as[10]

$$R_{\rm conv} = \frac{\delta}{k_{\rm c} \alpha S}, \quad (4)$$

where δ ($\approx 0.25 \times W_{\rm ch}$) is the thickness of the coolant boundary layer, $k_{\rm c}$ is the thermal conductivity of the coolant, α is the effective fin area multiplication factor ($\approx (2H_{\rm ch} + W_{\rm f})/(W_{\rm ch} + W_{\rm f})$), and S ($= W_{\rm total} \cdot L_{\rm ch}$) is the cooled size of the heatsink. The thermal conductivity of water is 0.61 W/(m·°C). The way to reduce $R_{\rm conv}$

is to increase H_{ch} and S and decrease W_{ch}. Increasing H_{ch}, however, will enlarge the thickness of the heatsink and reduce the packing density. W_{ch} and H_{ch} are also limited by the ability to machine the small, high aspect ratio channels. If the above-mentioned values of these parameter are used, then Eq. (4) yields $R_{conv} = 0.167$ °C/W.

The sum of R_{cond}, R_{heat}, and R_{conv} is 0.199 °C/W, which is the thermal resistance of a package unit. The 10-bar stack LDA comprises 10 package units and the thermal resistance is 0.0199 ◦C/W. When the device is operated at the 1200-W output power level, the dissipated power ΔQ at the junction is approximately 1200 W. From Eq. (1), we can get $\Delta T = 24$ °C. In the following, ΔT will be measured by monitoring the wavelength shift of the LDA. If the temperature of the coolant is 20 °C, then the temperature of the active region of the diode bar is 44 °C. At this junction temperature, the device can be efficiently and reliably operated.

The output characteristic of the LDA is shown in Fig. 3 with an inlet temperature of 20 °C. The inlet pressure and flow rate were 6.1×10^5 Pa and 160 cm^3/s, respectively. Limited by the current source, the maximum output power reached 1200 W at 120 A. Due to the excellent quality of the packaging technology, no thermal saturation was observed and the output power was perfectly linear with the drive current. The slope efficiency was 11.9 W/A over the full range. The spectrum width was 4 nm. The maximum conversion efficiency of 47.8% was achieved at 120 A.

The wavelength was 800.2 nm under the conditions of 10 Hz, 100 μs, 50 A, and it was 807.3 nm at CW 120 A. The wavelength shift was 7.1 nm. ΔT of 25.4 °C was calculated as a result of the coefficient of 0.28 nm/°C and the wavelength shift. The input power was 2376 W considering the operating voltage of 19.8 V and the operating current of 120 A. The output laser power was 1200 W, so the dissipated power was 1176 W. Thus we can obtain from Eq. (1) that $R_{th} = 0.0216$ °C/W.

Besides the achievable optical output power, one important figure for diode bars is the expected lifetime. Therefore, lifetime testing is an essential step of LD bar qualification. They are operated at constant driving current and their optical output power is monitored. When the output power has dropped by 20% of its initial value, 'end-of-life' is reached. From the observed degradation rate at the respective time intervals, the expected lifetime can be calculated.

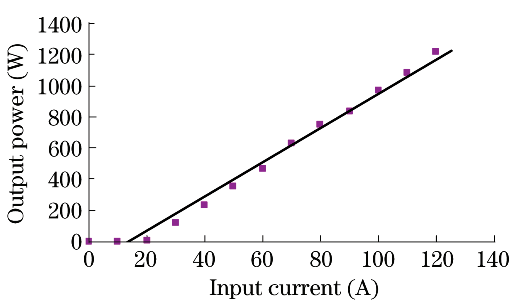

Fig. 3. Power-current characteristic of a 10-bar LDA under CW operation.

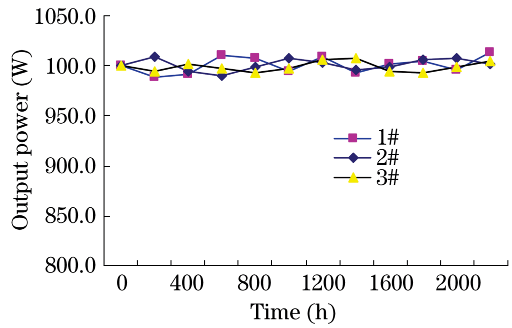

Fig. 4. Lifetime testing results of three LDAs.

The lifetime of 3 arrays were tested under constant operating current of 100 A at an ambient temperature of 20 °C. The lifetime data are plotted in Fig. 4. At 1000-W power level, the bars have run stably for 2200 h and shown an excellent degradation behavior. No sudden failure and no observable change at the operating current occurred.

In conclusion, a high packing density laser diode stack array has been developed utilizing Al-free active region laser bars with a broad waveguide and discrete copper microchannel-cooled heatsinks. The microchannel cooling technology leads to a stack LDA having very low thermal resistance and enables the device to be operated under CW condition at a high output power. The discrete copper heatsink is very thin and results in a high packing density and a small bar pitch. The reliability of the devices is enhanced due to the low temperature operation enabled by the small thermal resistance.

References

1. Y. Wan, K. Han, Y. Wang, and J. He, Chin. Opt. Lett. **6,** 124 (2008).
2. L. Fang and M. Zhao, Acta Opt. Sin. (in Chinese) **28,** (s1) 172 (2008).
3. M. Guo, J. Ki, W. Fu, X. Shi, Q. Hu, and W. Chen, Acta Opt. Sin. (in Chinese) **27,** 280 (2007).
4. Y. Feng, J. Meng, J. Bi, S. Du, J. Zhou, and W. Chen, Chinese J. Lasers (in Chinese) **35,** 1173 (2008).
5. P. Yan, S. Yin, and M. Gong, Chin. Opt. Lett. **6,** 580 (2008).
6. R. Beach, W. J. Benett, B. L. Freitas, D. Mundinger, B. J. Comaskey, R. W. Solarz, and M. A. Emanuel, IEEE J. Quantum Electron. **28,** 966 (1992).
7. J. A. Skidmore, B. L. Freitas, J. Crawford, J. Satariano, E. Utterback, L. DiMercurio, K. Cutter, and S. Sutton, Appl. Phys. Lett. **77,** 10 (2000).
8. R. E. Hendron, C. C. Becker, J. L. Levy, and J. E. Jackson, Proc. SPIE **1219,** 330 (1990).
9. D. B. Tuckerman and R. F. W. Pease, IEEE Electron Device Lett. **2,** 126 (1981).
10. D. Mundinger, R. Beach, W. Benett, R. Solarz, W. Krupke, R. Staver, and D. Tuckerman, Appl. Phys. Lett. **53,** 1030 (1988).